

⁸Y. Ballu and J. Lecante, to be published.

⁹For an incident electron beam traveling parallel to the surface, of current J per unit length normal to sur-

face, the total current scattered into a particular channel is $J\lambda$, where λ is the linear cross section for the channel.

Laser-Modulated Photoemission in Semiconductors

M. Wautelet and L. D. Laude

Faculté des Sciences, Université de l'Etat, Mons, Belgium

(Received 12 July 1976)

A novel, double-beam photoemission experiment is described in which electron energy distributions are obtained from semiconductors by modulating the ultraviolet photocurrent with a tunable, flash-excited, dye-laser beam. Double-beam photoemission spectra are demonstrated, in the case of tellurium, to result from optical transitions alone within the unperturbed bulk band structure of the solid. Unique information is obtained on the conduction-band-states distribution below vacuum level, within which a forbidden gap is demonstrated to exist between 2.5 and 4.7 eV above valence-band edge.

Information on the band structure of a solid is currently obtained from the interaction of a *single* electromagnetic beam with the solid.¹ However, this information may be shadowed by structural peculiarities resulting in uncertainties in the interpretation of the optical spectra. A more powerful way to investigate the electronic structure of a solid would be to associate two different optical-absorption processes initiated in the solid by two independent optical sources and to obtain an experimental evidence for such a coupling. The object of this Letter is to report on the results of an experimental inquiry which provides such an evidence and to demonstrate the advantage of the technique in terms of band structure.

The experiment uses basically a photoemission setup² in which a continuous uv beam and a pulsed, coherent beam are focused at 45° incidence onto the same ultrahigh-vacuum-cleaved crystal face. uv photons, of energy ϵ , initiate the excitation of valence electrons into the conduction band. These electrons are further emitted into vacuum, collected on a spherical analyzer, and contribute to the photoemission current, I . The coherent beam is provided by a Chromatix CMX-4 flash-excited dye laser in the 2–4-eV range. Pulses are delivered at adjustable frequencies, Ω_L , between 5 and 25 Hz. The total diameter of the beam is approximately 4 mm. The pulse power is 6 and 0.4 kW, corresponding to photon fluxes of 10^{16} and 3×10^{14} photons per pulse, at $h\nu_L = 2.08$ and 4.16 eV, respectively. Should a coupling take place within the solid between the uv photoemission process and the laser beam, an ac contribution to I would be produced at Ω_L . To obtain a detectable $I(\Omega_L)$ would require a laser beam such that the proportion between absorbed laser photons

and valence electrons behind the solid surface over a depth equal to l_e , the electron mean free path, be of the order of, at least, a few percent. Taking the valence-electron number to be about 10^{16} over, say, 20 Å, one sees that the laser used in this work does fulfill this mandatory condition. This ac current $I(\Omega_L)$ is selectively detected by passing I through a lockin amplifier phase-locked on Ω_L . The amplifier output is then stored in a multichannel signal analyzer. This output, namely the Ω_L derivative of $I(\Omega_L)$, represents the energy distribution curve (EDC) of *only* those emitted electrons which have "seen" both the uv and laser beams.

This double-beam photoemission (DBP) experiment, described here for the first time, has been tested on several semiconductors so far. Most impressive are the results obtained on (10 $\bar{1}$ 0) tellurium because of the distinct characteristics of its electronic structure. Therefore, some of the Te data will be presented in this Letter to demonstrate the unique advantages of the DBP technique. More complete Te data together with those on Ge, Si, Se, and others will be published elsewhere.

Two series of spectra have been obtained on (10 $\bar{1}$ 0) Te at $h\nu_L = 2.08$ and 4.16 eV in the 3.2–8.7-eV uv range. Some of these spectra are shown in Fig. 1, together with a (single-beam) EDC obtained at $\mathcal{E} = 7.71$ eV. In Fig. 1(b) at $h\nu_L = 2.08$ eV, one compares the 5.60- and 7.71-eV spectra; these have equal widths but show different profiles; in Fig. 1(c) at $h\nu_L = 4.16$ eV, the 7.71-eV spectrum is compared to the 3.51-eV one. The low-energy part of the 7.71-eV spectrum and the total 3.51-eV spectrum do compare well in width and position on the energy axis, differences ap-

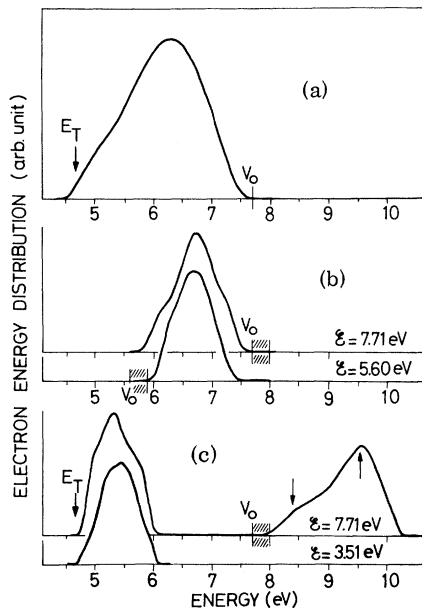


FIG. 1. (a) Classical (single-beam) EDC obtained from freshly cleaved (10 $\bar{1}$ 0) Te at $\epsilon = 7.71$ eV; and DBP spectra obtained for (b) $h\nu_L = 2.08$ eV and (c) 4.16 eV at uv energies separated by and energy equal to $h\nu_L$. In the DBP spectrum obtained at $h\nu_L = 4.16$ eV and $\epsilon = 7.71$ eV, the width of the high-energy part measures the width of the p_3 band. Shaded regions of the energy axis (measured from valence band edge) correspond to the p_2 - p_3 gap. Emission from valence-band edge is delineated by V_0 .

pearing again in the profiles.

A number of effects may contribute to the interpretation of these spectra. Second-order perturbations associated with the laser radiation field may be considered at first. According to the laser characteristics, this field is of the order of 10^{-2} - 10^{-1} V/m; it has been shown that for such a field magnitude the one-electron band structure of the solid³ is not modified significantly. Further, the pulsed laser beam may create a large number of free carriers near the surface and these could periodically neutralize the surface field. This quenching effect would induce a modulated band bending near the surface which would affect the whole band structure of the solid, as in a photorefectance experiment.⁴ Therefore, this would result in a classical EDC in contrast with actual observations, Fig. 1. Identical conclusions would apply to temperature-modulation effects, if any, induced by the laser on the sample surface. Most promising would be the fact that the DBP spectra might result from a modulation in the effective density of states produced by

electrons which are cooperatively excited into the conduction band via real or virtual intermediate states.

In particular so-called two-photon processes⁵ initiated by the absorption of laser-photon pairs via virtual intermediate states could be envisaged to account for the observed spectra. This would contribute an EDC extending from $E_T = 4.65$ eV to about 8.3 eV for 4.16-eV laser photons. In addition, such an EDC would not be sensitive to changes in the uv source energy. This is, by no means, observed in the actual spectra of Fig. 1. Therefore, an interpretation of DBP spectra is proposed in which cooperative excitation mechanisms involve *real* intermediate states only.

The Te band structure is essentially characterized by narrow bands. According to calculations,⁶ the valence band consists of two slightly overlapping bands, p_1 and p_2 , its total width being approximately 4 eV. Above a fundamental gap $E_G = 0.3$ eV, a first 2-eV-wide conduction band (p_3) would exist. A 2-eV gap would separate p_3 from a second (d -like) conduction band. The position of the latter has been adjusted² to fit the onset of p_2 - d optical absorption to the photoelectric threshold E_T [$E_T = 4.65$ eV for a freshly cleaved Te (10 $\bar{1}$ 0) face]. However, no experimental and direct proof of the existence and extent of the p_3 - d gap has been obtained so far. As suggested by the DBP spectra, (Fig. 1) it was foreseen that DBP could provide such an evidence.

Within the Te band structure, and due to the high laser-photon flux available, a large proportion of electrons might periodically populate p_3 , and, consequently, an equal number of valence states would be periodically depopulated at a rate equal to Ω_L . If uv photon absorption takes place from such periodically populated (p_3) or depopulated (p_1 or p_2) states, the energy distribution of those periodically uv excited electrons (i.e. the periodic component of the total energy distribution of the uv photoelectrons) would give evidence for three processes. Process 1 (Fig. 2) represents (i) the pulsed laser excitation of valence electrons from p_1 or p_2 states into p_3 states and (ii) the uv excitation of these once-excited electrons into d states after absorption of uv photons at energies ϵ_1 . Process 2 represents (i) as in process 1 and (ii) the uv excitation (at energies ϵ_2) of valence electrons the density of which has been modulated, through laser excitation. In addition, a *third* process may also appear (Fig. 2) due to the relative flatness of the Te bands. Excitation from deeper valence states could occur

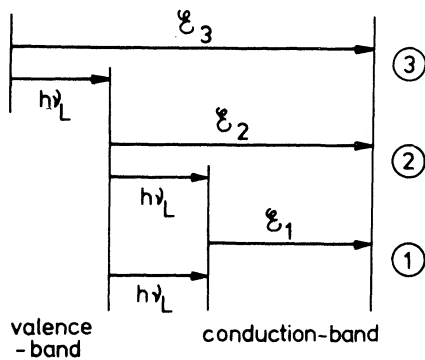


FIG. 2. Schematic representation of the three co-operative excitation processes discussed in text. If a d state is periodically populated via process 1 at uv energy ϵ_1 , it may also be periodically populated via process 2 at energy $\epsilon_2 = \epsilon_1 + h\nu_L$ and might do so via process 3 at energy ϵ_3 , only if $\epsilon_3 = \epsilon_1 + 2h\nu_L$.

by absorption of $h\nu_L$, into higher valence states which are already periodically depopulated. Modulated uv optical excitation could take place from such deep valence states by absorption of uv photon energies $\epsilon_3 = \epsilon_2 + h\nu_L$.

A search for the d states which could be periodically populated via process 1, 2, or 3 has been made through the band structure calculated by Maschke using the pseudopotential method.⁶ According to this band structure, the energy distributions of these periodically populated conduction-band states, measured from valence-band edge, are obtained at $h\nu_L = 2.08$ [Fig. 3(a)] and 4.16 eV [Fig. 3(b)]. At a given uv photon energy, a set of such conduction states is obtained. Each of them occupies an energy level E which is represented by a point on the horizontal energy scale of Figs. 3(a) and 3(b). These points contribute the structure of theoretical energy distribution curves which may be calculated formally within the three processes involved. Note that, according to Fig. 3, identical structural features would appear in spectra obtained at uv energies ϵ and $\epsilon + h\nu_L$. Intensity of such features would however vary with transition matrix elements.⁷

As read on the 45° axis (or initial-state energy scale), contributions of processes 1 and 2 to the DBP spectra should have a maximum width equal to $(h\nu_L - E_c)$. This is actually the case at $h\nu_L = 2.08$ eV [Fig. 3(a)] and is *not* the case at $h\nu_L = 4.16$ eV [Fig. 3(b)], stemming from the presence of a forbidden gap within the conduction-band states distribution, between $E = 2.5$ and 4.7 eV, above the valence-band edge. Therefore, at $h\nu_L = 4.16$ eV, the maximum width of processes

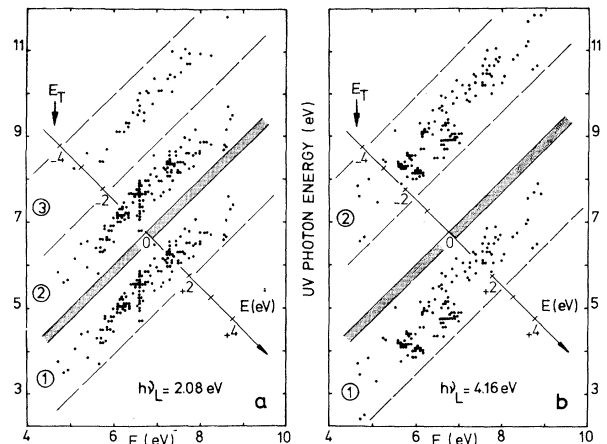


FIG. 3. Energy distribution above valence-band edge (abscissa) of structural features (points) appearing in DBP spectra, as obtained from Te band structure (Ref. 6), through the three processes of Fig. 2, at (a) $h\nu_L = 2.08$ eV and (b) $h\nu_L = 4.16$ eV. Points can be located on the 45° axis on which energies are obtained from the final-state energy E (read on abscissa) minus the uv photon energy quoted on the vertical axis. Shaded areas represent the region of the diagrams corresponding to the (p_2-p_3) gap. Oblique dashed lines delineate regions contributed by each single process (Fig. 2). The structure of every experimental spectrum (Fig. 1) should compare to the horizontal points distribution appearing at the same uv (ϵ) and laser ($h\nu_L$) energies.

1 and 2 contributions would be equal to the width of the so-called first conduction band p_3 . In addition, at uv energies below $\mathcal{E} = 8.6$ eV, the low-energy onset of all energy distribution [Fig. 3(a) and 3(b)] would delineate emission from states near the bottom of a second (d -like) conduction band. The evolution of these theoretical energy distributions (Fig. 3) with uv and laser energies do compare very well with those observed on experimental DBP spectra, as seen in Fig. 1.

At $h\nu_L = 2.08$ eV, the $\mathcal{E} = 7.71$ -eV spectrum is confined between $E = 5.8$ and 7.7 eV and is contributed by process 2 only, while the spectrum obtained at $\mathcal{E} = 5.60$ eV (or $7.71 - h\nu_L$) extends over approximately the same energy range but is due to process 1, Fig. 3(a). Differences in the profiles of these two spectra may be considered as a direct evidence for the effect of the matrix elements, since in both cases the same d -band states are populated via different intermediate states, Fig. 2.

At $h\nu_L = 4.16$ eV (Fig. 1), the low-energy part (contributed by process 2) of the 7.71-eV spectrum and the 3.51-eV (or $7.71 - h\nu_L$) spectrum (due to process 1), extend both between $E = 4.7$

and 6.0 eV, again with differences in the respective profiles attributed to matrix elements. According to Fig. 3(b), process 1 appears to contribute the high-energy part of the 7.71 eV, extending from $E = 8.0$ to 10.2 eV. Note the two features centered at $E = 8.5$ and 9.6 eV, respectively. The latter is not described in Fig. 3(b) since the band structure actually used extends up to $E = 9$ eV only. This peak gives evidence for additional states distributed at $E > 9.0$ eV, i.e., just above the d band. They are populated here up to $E \approx 10.2$ eV through process 1, initiating at $E \approx -1.7$ eV via states lying at $E \approx 2.5$ eV. If this level delineates the high-energy edge of p_3 , the upper limit of process 2 contribution to the spectrum should be located at $E = 10.2 - 4.16 \approx 6.0$ eV, which is quite precisely observed [Fig. 3(b)]. The upper limit of the 3.51-eV spectrum is around $E = 6.1$ eV which corresponds (via process 1) to a p_3 level at $E = 6.1 - 3.51 \approx 2.6$ eV, in agreement with the 7.71-eV spectrum. This sets for the first time the upper edge of p_3 , in close agreement with calculations.

Altogether, the present experiment confirms the band structure of Maschke.⁶ It brings unique information on the width of p_3 and the upper-lying conduction-band states. Worth noting is the fact

that the above experimental data are *not sensitive* to surface aging, i.e., information therein obtained is characteristic of the bulk electronic structure.

The authors gratefully acknowledge valuable discussions with Professor A. A. Lucas, with regard to Ref. 3, and Dr. B. Kramer and the expert technical assistance of J. P. Toubeau.

¹See, for instance, M. Cardona, *Modulation Spectroscopy*, Suppl. No. 11 to *Solid State Physics*, edited by H. Ehrenreich, F. Seitz, and D. Turnbull (Academic, New York, 1969).

²L. D. Laude, B. Kramer, and K. Maschke, *Phys. Rev. B* **8**, 5794 (1973).

³N. Tzoar and J. I. Gersten, *Phys. Rev. B* **12**, 1132 (1975).

⁴R. E. Nahory and J. L. Shay, *Phys. Rev. Lett.* **21**, 1569 (1968).

⁵E. M. Logothetis and P. L. Hartman, *Phys. Rev.* **187**, 460 (1969).

⁶K. Maschke, *Phys. Status Solidi* **47**, 511 (1971); B. Kramer, K. Maschke, and L. D. Laude, *Phys. Rev. B* **8**, 5781 (1973).

⁷The effects of transition matrix elements are better evidenced in germanium (L. D. Laude and M. Wautelet, to be published).

X-Ray Photoelectron Spectroscopy of the Intermediate-Valence State in the $\text{EuRh}_{2-x}\text{Pt}_x$ System

I. Nowik,* M. Campagna, and G. K. Wertheim

Bell Laboratories, Murray Hill, New Jersey 07974

(Received 20 October 1976)

By considering the results of Mössbauer studies and x-ray photoelectron spectroscopy, we obtain a phenomenological model of the intermediate valence state in the homogeneous system EuRh_2 . The interconfiguration excitation energy is 1550 ± 150 K, and the mixing width, 2Δ , is 0.10 ± 0.02 eV. In $\text{EuRh}_{2-x}\text{Pt}_x$ the Eu valence is determined by the local environment, including neighbors beyond the nearest shell.

The intermediate valence phenomenon¹ has most often been investigated by measurement of static (adiabatic) parameters, e.g., the unit cell, conductivity, thermal properties, susceptibility, and Mössbauer spectra. However, only measurements in the sudden or high-frequency limit can reveal the electronic configuration involved in the fluctuations. This distinction has often been related to the "measuring time" of the technique compared to the fluctuation time² τ_f of the system. In this picture the time scale of Mössbauer spectroscopy is set by nuclear lifetime and hyperfine frequencies, typically 10^{-11} sec, which,

as we shall show, are long enough so that only an average state is observed. It is generally recognized that the measuring time in x-ray photoelectron spectroscopy (XPS) is of the order of 10^{-17} sec. However, it introduces a large perturbation by the removal of one electron. Nevertheless it is of great interest to study by XPS systems which have been found by other techniques to be in an intermediate valence state. Such studies have been conducted with systems containing Sm and Tm ions.³ SmB_6 has been studied by the Mössbauer technique,^{4,5} showing definitely an isomer shift which lies between that of